OPEN WATER CHARACTERISTICS OF THREE MODEL SCALE FLEXIBLE PROPELLERS

Luca Savio [*†] **and Kourosh Koushan**[*†]

[*] Department of Ship and Ocean Structures
SINTEF Ocean
Trondheim, Norway
e-mail: Luca.Savio@sintef.no , web page: https://www.sintef.no/ocean/

[†] Department of Marine Technology
Norges teknisk-naturvitenskapelige universitet (NTNU)
Trondheim, Norway
e-mail: kontakt@marin.ntnu.no - Web page: https://www.ntnu.edu/imt

Key words: Experimental Hydrodynamics, Marine Propellers, Static Hydroelasticity

Abstract. In this paper the experimental setup, the data analysis procedure and some results of a series of tests on 3 propeller blade designs that aimed to provide validation data for static hydroelastic computations are discussed. The propellers were produced both in a rigid and in a flexible variant so that the effect of elasticity of the material could be studied.

1 INTRODUCTION

The hydroelastic behavior of propellers has been a recurring topic in ship propulsion; seen at time as a possible cause for failures of propulsive systems and some other times as an opportunity for improving the performances of propellers as a noise and vibration sources, it often suffered from a lack of experimental material to validate design and analysis codes. There are, as a matter of facts, very stringent limitations on what can be done in experiments on propeller models in hydrodynamic facilities. These limitations arise both from the scaling laws the experiments abide to and from the difficulties in producing flexible, with controlled mechanical properties, propeller blades. However, the progresses in computer simulations of fluids and structures allow for another strategy to be sought. In fact, it is possible to use the numerical simulations as a link between the model scale experiments, where the test conditions can be accurately controlled, and the full scale products, which is where hydroelasticity ultimately matters. The strategy, that is often used in hydrodynamics, is to validate the codes in model scale, in this way ensuring that can be used to simulate full scale phenomena.

In this paper we present the results from a series of tests carried out on three homogeneous and isotropic flexible propeller blade sets. The three propellers are variations of the same geometry, where the original blade skew distribution was altered. The blades were produced both in

aluminum and in a epoxy-like resin, through the technique of resin casting. The aluminum blades served to make the form for the resin blades, and as a reference as rigid blades since their elasticity can be neglected in model scale. The tests were carried out in SINTEF Ocean's large towing tank in open water condition, i.e the inflow to the propeller was uniformly distributed. The tests were performed at different propeller rotational speeds and at different pitch settings. In order to establish a reference condition for the flexible propellers, all the tested conditions were also run with the rigid blades; in this way, it was possible to quantify the significance of the different Reynolds number at which the blades were tested. It is worth pointing out that the terms rigid and flexible are used here to refer to the blades made of aluminum and resin respectively; in fact, even-though also the aluminum blades are strictly speaking flexible, their stiffness in model scale makes any deformations under the effect of hydrodynamic loads too small to be observable; on the contrary, the resin blades clearly show deformation when loaded that can be measured by the laboratory equipment.
Care was taken not to excite any resonance in the blades. Furthermore, since the inflow was homogeneous, the response of the blades was static. Becuase of the lack of any dynamics, the tests presented here fall under the category of static hydroelasticity.

1.1 Symbols used in the paper

The following non dimensional numbers will be used in the paper.

$$J = \frac{V}{nD} \tag{1}$$

$$K_T = \frac{T}{\rho n^2 D^4} \tag{2}$$

$$K_Q = \frac{Q}{\rho n^2 D^5} \tag{3}$$

$$\eta_O = \frac{J}{2\pi}\frac{KT}{KQ} \tag{4}$$

where J is the advance number, K_T the thrust coefficient, K_Q the torque coefficient and η_O the propeller efficient. Further, V [m/s] is the advance speed , n [rps] is the rotational speed or shaft speed , D [m] is the diameter and P [m] the pitch of the propeller ; T [N] is the thrust delivered by the propeller and Q [Nm] the torque absorbed by the propeller. The suffixes A and R indicate the data relative to the aluminum and resin propeller respectively.

2 GEOMETRY DEFINITION AND MODEL PRODUCTION

When referring to hydro-elasticity of propellers it is common to think of the so called bend-twist coupling of composite blades. Bend twist-coupling is phenomenon by which a structure that is bent in spanwise direction shows also some twist of the sections perpendicular to the direction of bending. In marine propellers, one typical application of bend-twist coupling is to create a blade structure that reduces the pitch by structural response when subjected to a load increase. The most common way of obtaining such a de-pitching effect under increased load is to use composites materials with an ad-hoc ply orientation sequence. However, bend-twist coupling

exists also for isotropic and homogeneous lifting surfaces when the center of pressure in away from the elastic axis of the structure. In principle it is possible to control bend-twist coupling of isotropic blades by changing the relative location of the blade elastic axis and the center of pressure, for example by acting on the skew distribution. However, it has to be remarked that the blade skew distribution is determined by considerations regarding cavitation and hence it is very unlikely that the skew distribution can be used for controlling the hydroelastic behavior of marine propellers. Nevertheless, for research purposes, using the skew distribution is a straightforward strategy to generate blades that have a different elastic behavior starting from the same parent geometry. The propeller geometries that will be presented in the next paragraph were designed within the framework of the project PROPSCALE for studying numerically the effects of Reynolds number on the open water curves of marine propellers. The three geometries are identical a part from the skew distribution; for this reason they were perfect candidates for the purpose of generating flexible model scale propellers that show different hydroelastic behaviors.

2.1 Geometrical definition of the propellers

The parent propeller geometry from which the other geometries were derived is P1374 whose geometry is public and a large amount of numerical and experimental data is available. Propeller P1374 was designed by SINTEF Ocean using the design code AKPD/AKPA as a propeller to be used for research purposes; it was, therefore, straightforward to generate variations of the original geometry.

Propeller P1374 has a total skew of 23 degrees distributed in a balanced way. The first variation, P1565, was obtained by removing the skew completely and the second, P1566, by abandoning the balanced skew design for an almost linear distribution. The skew distribution of the 3 geometries is shown in Figure 1; the skew is given in mm, according to the geometry definitions used by AKPD/AKPA.

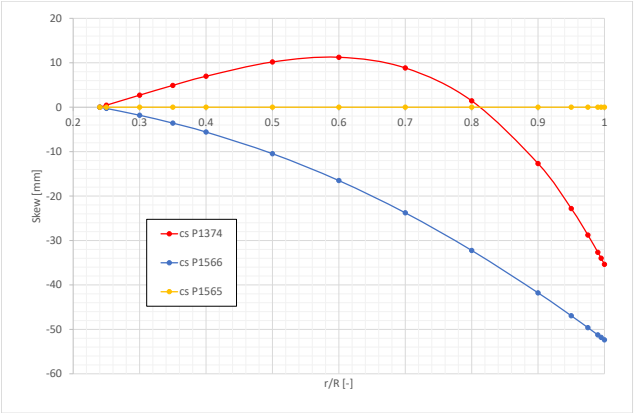

Figure 1: Comparison of the skew distribution for the 3 geometries

3

The silhouette of the blades depicted in Figure 2 offers a visual impression of the differences between the three designs.

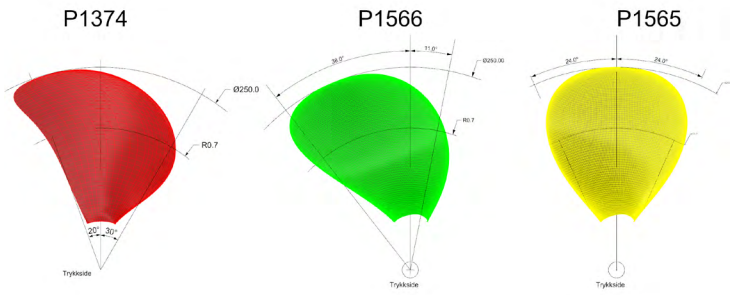

Figure 2: Silhouette of the blades of propellers P1374, P1565 and P1566

2.2 Production method for the flexible propellers

The propeller blades that are used in model testing are often produced in a metallic material, such as aluminum or bronze, with the latter being the most common, in order to limit the deformations during testing. It is not often that the blades need to show a measurable deformation in model scale, and hence there is no standard practice on how to produce them. Several techniques may be employed, as for example, 3D printing, milling and resin casting. After some considerations on the advantages and disadvantages of the different options, it was chosen to use the resin casting technique

At first glance 3D printing may appear the most appealing technique because it is fast and relatively inexpensive. Almost any geometry, even hollow geometries, can be produced with no added complexity to the production process. However, the homogeneity and isotropy of the material properties of the printed object are a matter of discussion in the scientific community, and have not being addressed until recently when 3D printing was no longer only adopted in prototyping but also in production. Test performed in the HyDynPro project showed that, at least for the printer that was used in that case, the printing material was rather homogeneous, unless the printing process completely failed. Nevertheless, given the lack of certainty on whether the material could be considered isotropic or not, it was decided to abandon this option.

Propeller models may also be milled out of a block of raw material that has the desired mechanical properties, ensuring that the material is homogeneous and isotropic. The list of

materials that can be used is much larger than that can be used with any of the other proposed techniques. Milling, in addition, is the process that is used for metal propellers and hence it may be foreseen that most of the same production technique can be utilized. However, some aspects have to be pointed out; first, milling plastic materials is rather different from milling metal, it requires experience and some rethinking of the manufacturing process; second, the production process through milling requires some manual work since some parts cannot be reached by the cutting tool, the result of hand work on plastic may be rather different from the one obtained with on the metal propeller. Since milling turned out to be not as straightforward as it may have looked at first glance, it was abandoned.

Resin casting was the last technology to be evaluated, but was in the end selected because, at least in this specific case, it is rather cheap and has reasonably short production times. The resin casting process starts with the production of a plastic mold, made of silicon, that is obtained from a template; the mold is, therefore, a negative copy of the template which is therefrom called a positive. In the silicon mold it is then cast a specific resin that is left to cure in a vacuum chamber, where the temperature is kept constant. There are two main restriction to resin casting: the selection of materials and the need of a positive template. As far as the selection of materials is concerned, the range of mechanical properties that the different resins offer is not very wide; in fact, most of the casting materials have a Young's modulus in the range 2-4 GPa. The need of the positive template may be a drawback if only the flexible object is needed; luckily, for this project also the metallic propeller was needed and hence no extra cost was incurred to make the positive template. In case just the flexible propeller blades are needed, the cost of making the positive metallic template would be significantly higher than the cost of the flexible blades.

The resin blades were manufactured by a company that specializes in rapid prototyping, PROTOTAL A.S, using a casting resin type 8051 produced by MCP HEK Tooling GmbH. The main mechanical properties of the material are reported in Table 1 . The reported data are taken from the data sheet, i.e. no independent test was carried out to confirm them. The Poisson's ratio is not specified by the producer, but given the nature of the material, can be assumed to be 0.33.

Table 1: Main mechanical parameters of the adopted resin

Tensile E-Modulus	2150	MPa
Tensile Strength	55.9	MPa
Flexural E-Modulus	1965	MPa
Flexural Strength	85.9	MPa
Specific Gravity Part A	1120	kg/dm3
Specific Gravity Part B	1190	kg/dm3

3 SETUP AND EXECUTUTION OF THE TESTS

3.1 Test setup

The tests were carried out using the standard test setup used for open propellers in the towing tank. In the standard setup the propeller is placed in front of the dynamometer that is mounted to the towing carriage. The forward motion of the propeller is that of the towing carriage, while the rotational speed is set by an electric motor that drives the propeller shaft. For any given combination of propeller speed and carriage speed the thrust generated and the torque adsorbed by the propeller are measured. The propeller is mounted on the dynamometer as Figure 3 shows; it is important to note that only the forces generated on the left side of the 1mm gap visible in the figure are measured by the dynamometer.

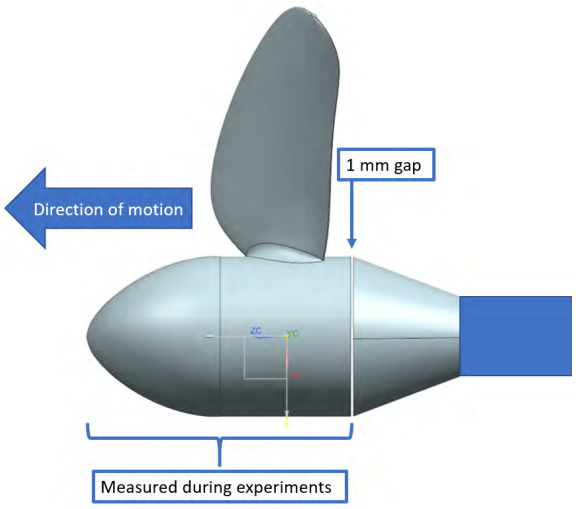

Figure 3: Propeller setup on the dynamometer

Traditionally, when the tests are carried in the configuration described in this paragraph, a test at various advance and rotational speeds with a dummy hub (instead of the propeller) and the propeller cap is carried out to measure the resistance of the hub and cap. The measured resistance is then subtracted from the measurement carried out with the propeller to constitute what is the traditionally reported as the propeller open water. Also in this case the correction test was carried out and the data are available both with and without the correction. The uncorrected data should be used anytime it is possible to integrate the force on the entire surface the is on left side of the 1mm gap; this is always the case for CFD codes, for example, and therefrom the double presentation of the data.

3.2 Test conditions and execution

The same set of tests were carried out on all propellers, rigid and flexible, and comprised variations in pitch setting (P/D), rotational speed and advance coefficient. In addition to the design pitch ratio (1.1) a reduced pitch (0.9) and an increased pitch (1.2) were tested. The

propellers were tested at the rotational speeds 7, 9 and 11. The advance coefficient was varied in steps that were defined based on the pitch settings as Table 2 lists.

Table 2: Advance coefficients as a function of the pitch setting

P/D 0.9	**P/D 1.1**	P/D 1.2
0.15	**0.2**	0.225
0.3	**0.4**	0.45
0.45	**0.6**	0.675
0.6	**0.8**	0.9
0.75	**1**	1.125
0.9	**1.2**	1.35
1.05		

In total 905 measurements were performed during the experimental campaign. In order to limit viscoelastic effects in the material, the test conditions were chosen so that the material would not be loaded more than 1/3 on its tensile strength limit. Finite element computation were carried out to check the stress levels in the material.

The tests were conducted in the following way. First, the propeller revolutions (rps) were adjusted to the desired value while the carriage was standing still. Then, the carriage speed was varied in steps until the maximum J value for the given condition was reached. The recording time between the steps was 10 seconds.

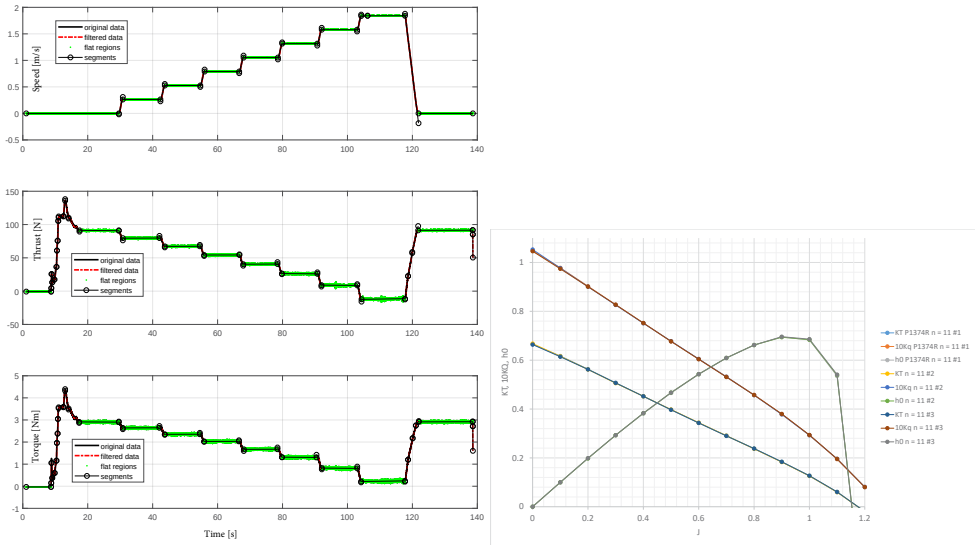

Figure 4: Example of a time series from the tests (left) and of the results from repeated runs (right)

Figure 4 left shows a typical test where the carriage speed was stepped through the different

advance coefficients from zero speed (bollard pull) to the maximum speed, that coincided to negative propeller thrust. The figure shows as green segments the parts of the signals that have been identified as stable and flat regions of the signal over which the average values are computed . A region of signal is considered to stable and flat if it can be approximated as a segment that has the absolute value of the slope (rate of variation) lower than a given threshold. The threshold for the slope of the carriage speed was set to $0.01m/s$, for thrust to $0.1N/s$ and to $0.01Nm/s$ for torque. Compared to the values that are normally accepted, the threshold for thrust was higher than usual. The higher value for the threshold of propeller thrust may indicate that some visco-elastic creep in the material was present. In order to check whether the blades underwent significant visco-elastic deformations, at the end of every run a bollard pull run is recorded to be compared to the one at the beginning of the run. With reference again to Figure 4 left, it can be seen that the propeller thrust and torque at the end of the run match those at the beginning of the run. In addition, for the flexible blades, the each condition was repeated three times. In Figure 4 right, the three repetitions for the same propeller are shown on the same graph; the high repeatability of the tests, witnessed by the fact that the curves are indistinguishable, is a good indication that the blades were nor temporarily nor permanently deformed.

4 DATA ANALYSIS AND EXPERIMENTAL UNCERTAINITY

4.1 Data Analysis

From the data recorded during the experiments, the average values over the flat regions were extracted as shown in Figure 4. When more than one run was available for the same propeller configuration and J value, which we will call from now on a condition, the average of the average values was computed. Once a single value per condition was obtained, the values were interpolated by fifth order polynomials. An example of the data fitting is shown in Figure 5 where the dots are the measured data and the lines the fitted polynomials.

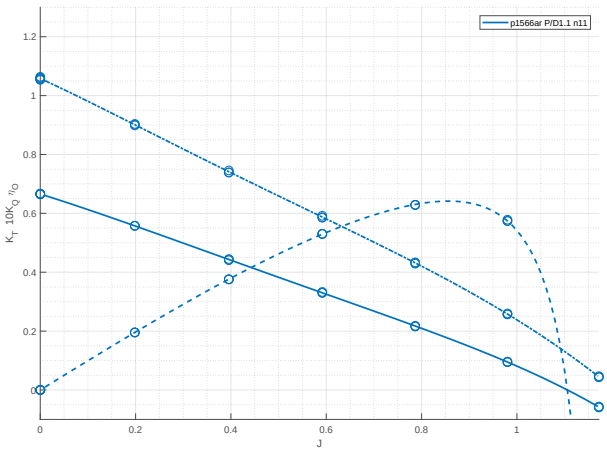

Figure 5: Curve fitting to the data

4.2 Evaluation of experimental uncertainty

The uncertainty of the experiments has been evaluated according to the type B evaluation as described by the GUM [1] standard. In the evaluation the sources of uncertainty that were considered are relative both to the measurement chain and to the propeller geometrical conformity. The relative experimental uncertainty has been found to be in the order of magnitude of 3% and increasing for high J values.

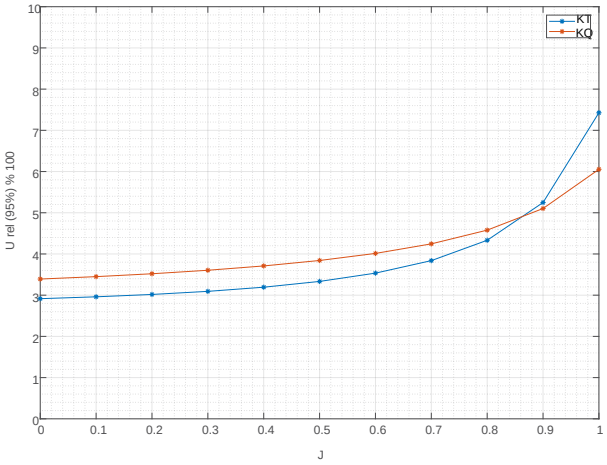

Figure 6: Relative uncertainty for n=7 rps

Figure 6 reports a typical relative uncertainty plot for n = 7 rps; this rotational speed is considered the worst case scenario as the measured forces are the lowest of the three speeds tested.

5 DATA PRESENTATION

It is not possible to present here all the data that were collected in the tests, but they can be made available upon request, both as raw measured data or as interpolating polynomials. In both cases the data are presented both with and without correction for the hub and cap resistance.
Several of expected features that have been observed in the data will be briefly described here in order to show how rich is the data set in terms of validation material.
The tests were performed for each propeller at different rotational speed also for the metallic version. It is expected that the efficiency of the propeller increases with the increasing Reynolds number; this well-known Reynolds effect can be seen in Figure 7 for one of the metallic propellers.

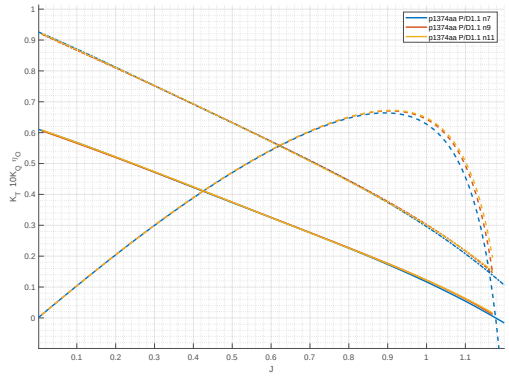

Figure 7: Reynolds effect of the open water curves

The effect of the different skew distributions of the three propeller designs can be seen in Figure 8 where the open-water curves of the three aluminium propellers are compared at the same pitch and shaft speed.

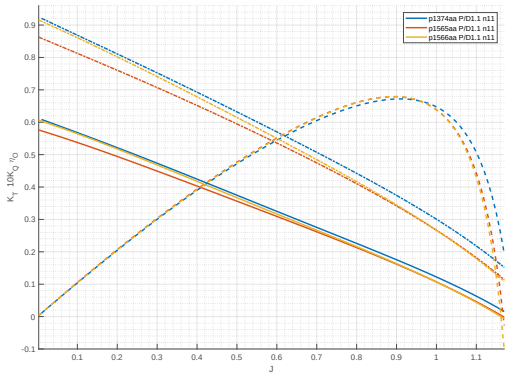

Figure 8: Effect of skew distribution

Because the inflow to the propellers was homogeneous, the resin blades showed a static response to the hydrodynamic load. Albeit the deformations were not measured, the increase of the thrust and torque coefficients of the resin blades compared to their metallic variant indicates that the blades were surely twisted in radial direction as Figure 9 shows.

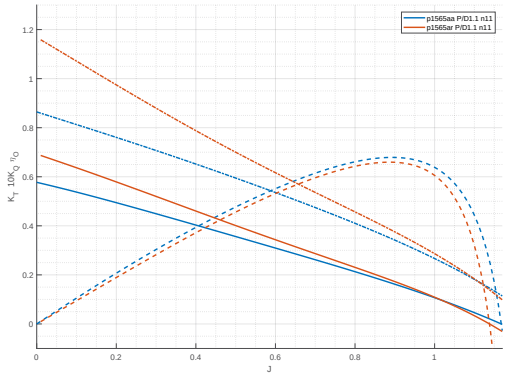

Figure 9: Comparison of open-water curves for the same propeller in metal and resin

The effect of the shaft speed, that translates into propeller load, on the blade twist can be clearly seen in Figure 10 where left to right the difference between the flexible and the rigid thrust coefficient $\delta K_T = K_{TR} - K_{TA}$ at the different shaft speeds is presented for the geometries P1374, P1565 and P1566, respectively.

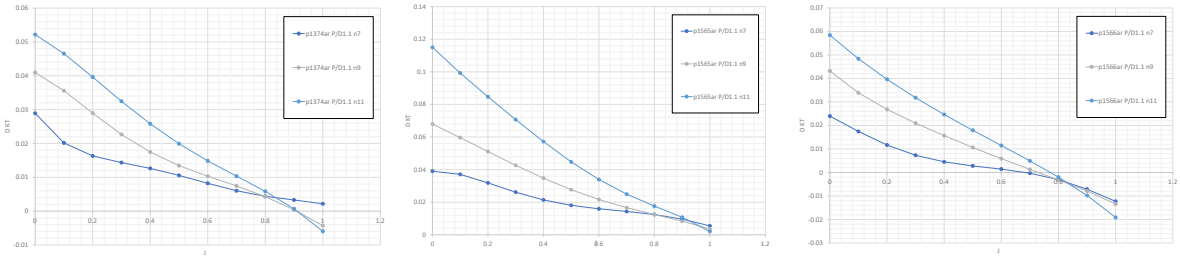

Figure 10: Effect on the propeller loading on the twist of the blades

The difference in thrust coefficient δK_T increases for J values lower than the J of maximum efficiency, while it decreases for higher values of J. Propellers are designed to operate with optimal angles of attack around the J of maximum efficiency. For J values lower than the design one, the angles of attack are increasing with decreasing J values, while the opposite happens for J values that are higher than the design one. In both cases the relative position of the pressure and section shear centers changes, resulting in a varying twist of the blade in radial direction dependent on the J value. From Figure 10 it can be seen that the all three geometries tend to show little twist in the J range from 0.8 to 0.9, i.e. close to the design point. The blade twist results in a global pitch increase for advance coefficients lower than the design point and decrease for advance coefficients higher than the design one. Furthermore, a closer look to the three graphs reveals that there are clear differences in how the different designs behave in relation to variation in load. The relation between thrust coefficient change and J value is compared for the three propellers for n = 11 rps in Figure 11. The reason why the three blade respond differently to changes in J values is twofold, but both reasons relate to the skew distribution.

The first reason is that the skew distribution changes quite significantly the open-water curves as already shown in Figure 8. The second reason is that, as mentioned in the second paragraph, the skew distribution changes the elastic axis of the blade.

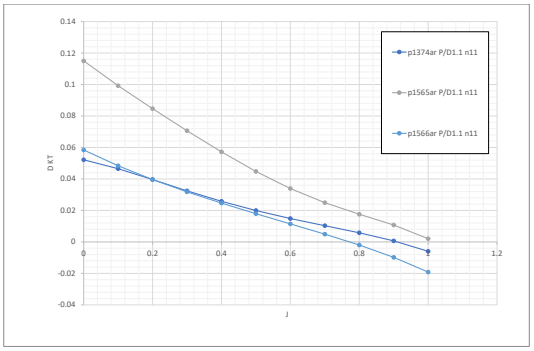

Figure 11: Comparison of the different J to relative KT for the three designs at n=11 rps

6 CONCLUSIONS

The measurements performed on three propeller designs that were produced both in aluminium and resin have been presented. The tests were performed at different P/D settings and propeller shaft speed in open water condition in SINTEF Ocean large towing tank. The geometries of the propellers and the data from the tests can be obtained upon request.
The tests aimed to provide validation material for numerical simulations of the static hydroelastic response of marine propellers. The test matrix is wide enough to allow validating design and simulation codes against the effect of the Reynolds number, the effect of skew distribution on the open-water curves of rigid propellers and the static hydroelastic response of the resin propellers. The tests presented here are part of the FleksProp project that intends to establish better design practices for the marine flexible propulsors, thus including not only propeller, but also thrusters. Within the scope of the project also composite propellers will be investigated and the interaction of the propeller with the thruster body will be considered too.

7 ACKNOWLEDGEMENTS

The present work has been fully supported by the FleksProp project. The FleksProp project is cooperation between SINTEF Ocean, the Norwegian University of Science and Technology NTNU and Rolls Royce Marine with the economic support of the Research Council of Norway (RCN) and Rolls Royce Marine. The economic support of the Research Council of Norway and Rolls Royce Marine is greatly appreciated.

REFERENCES

[1] JCGM 100:2008 GUM 1995 with minor corrections - valuation of measurement data — Guide to the expression of uncertainty in measurement

[2] Atkinson, P. & Glover, E.J. (1988). 'Propeller hydroelastic effects'. Propellers 88 Symposium, Virginia Beach, Virginia, September 20-21, 1988.

[3] Savio, L.(2015): Measurements of the deflection of a flexible propeller blade by means of stereo imaging. SMP2015 - The Fourth International Symposium on Marine Propulsors; 2015-05-31 - 2015-06-04

[4] Yin L. Young, Nitin Garg, Paul A. Brandner, Bryce W. Pearce, Daniel Butler, David Clarke, Andrew W. Phillips, Load-dependent bend-twist coupling effects on the steady-state hydroelastic response of composite hydrofoils, Composite Structures, Volume 189, 2018, Pages 398-418, ISSN 0263-8223, https://doi.org/10.1016/j.compstruct.2017.09.112.

[5] Achkinadze, A.S., Krasilnikov, V.I. (1999). 'A Numerical Lifting-Surface Technique for Account of Radial Velocity Component in Screw Propeller Design Problem. Proceedings of the 7th International Conference on Numerical Ship Hydrodynamic NSH7, July 19-22, Nantes, France.

[6] Achkinadze, A.S., Krasilnikov, V.I. and Stepanov, I.E. (2000). 'A Hydrodynamic Design Procedure for Multi-Stage Blade-Row Propulsors Using Generalized Linear Model of the Vortex Wake. Proceedings of the Propellers/Shafting'2000 SNAME Symposium, Virginia Beach, VA, September 20-21.